EFFECT OF ARTIFICIAL CRACK ASPECT RATIO ON TENSILE AND COMPRESSIVE PROPERTIES OF WELDED API X70 STEEL

BY

ERINFOLAMI, Isaac Oluwatominiyi
(M.ENG/SEET/2017/6726)

A THESIS SUBMITTED TO THE POSTGRADUATE SCHOOL,
FEDERAL UNIVERSITY OF TECHNOLOGY, MINNA IN PARTIAL
FULFILLMENT OF THE REQUIREMENTS FOR THE AWARD OF MASTER
OF ENGINEERING DEGREE IN MECHANICAL ENGINEERING
(INDUSTRIAL AND PRODUCTION OPTION)

NOVEMBER, 2021

ABSTRACT

Pipelines are joined by welding and are used for transportation of oil and gas products globally. These joints are prone to surface defects and sometimes deep cracks depending on types of loading they experience while in operation. Hence, it is necessary to understand the effect of defects on mechanical properties of welded pipeline joints to estimate their service lives. In this study, both experimental and numerical approaches were used to study the effects of aspect ratio on pipeline integrity. Artificial cracks were created on API X70 steel tensile and compression specimens using different aspect ratios. Universal Testing machine was employed in carrying out the experimental and ANSYS 2019 2R was used for modelling and loading of the specimens. Results show that the investigated mechanical properties were not only sensitive to materials type (weld and base) but also to aspect ratio. The tensile maximum stresses for experimental and numerical result for plain and weld materials without artificial crack aspect ratio was determined to be 706.8 MPa and 1176.9 MPa for plain materials, while 667.8 MPa and 646.92 MPa for weld materials respectively. The compression strength was 1200.4MPa and 1300.2 MPa for plain, while for weld 1393.7 MPa and 1902.1 MPa respectively. For specimens with artificial crack aspect ratios, tensile results are 706.8 MPa and 1776.9 MPa for Plain at aspect ratio of 0.2 respectively, while weld are 667.8 MPa and 646.93 MPa at aspect ratios of 1.0 and 0.2 respectively. That of compression were 1238.5 MPa and 1637.9 MPa at aspect ratios of 1.0 and 0.2 for plain, 1500.5 MPa and 1929.9 MPa at aspect ratios of 1.0 and 0.2 respectively. The maximum stresses obtained for tensile and compression specimens with or without artificial crack aspect ratios were discussed.

Table of Contents

LIST OF FIGURES

LIST OF PLATES

LIST OF ABBREVIATIONS

ABBREVIATION

API	American Petroleum Institute
TMCP	Thermo Mechanical Control Process
TM	Thermo Mechanical
HSLA	High Strength Low Alloy Steels
ASTM	American Standard for Testing Material
SMAW	Shield Metal Arc Welding
GTAW	Gas Tungsten Arc Welding
NDT	Nondestructive Testing
ACC	Accelerated Cooling Condition
DIFT	Deformation Induced Ferrite Transformation
SIF	Stress Intensity Factor
EBSD	Electron Backscatter Diffraction

CHAPTER ONE

1.0 **INTRODUCTION**

1.1 **Background to the Study**

Pipelines are generally used for the transportation of natural resources and fluids such as oil and gas over a long distance which use over the years have been extended to the transportation of potable and industrial chemical products, water, sewage and even solid materials like coal and ores (Wang *et al.,* 2014). The significant demand for oil and gas products necessitate the transportation of the production over a long distance for the crude oil reservoirs through the refining facilities to where they are demanded (Wang *et al.,* 2014). These pipelines which have been subjected to deterioration over the years due to several factors such as third-party damage, manufacture and materials defects, corrosion and natural forces (Shamsuddoha *et al.,* 2013)

As new steels are being produced with well-defined mechanical properties which gives relevant information on the behavior and characteristics as used in construction, transportation and almost all engineering application. Due to new damage mechanisms as more advanced applications with diverse mode of operations and environmental factors are created, it then nullifies the statement that behaviour and characteristic of construction materials is known.

In the early 1960s, medium carbon steel were the materials employed in line pipe industries; but with the technological improvement and development in welding processes, use of microalloying element in steel and thermo mechanical control process (TMCP) have enabled the industry in producing high-strength steel (Natividad *et al.,* 2017). For some times now there has been an increase in demand for increasingly larger pipe diameters, higher operating pressure and diversity of products transported by the

pipeline industry (Ike *et al.,* 2018). In order to avoid large wall thickness, higher strength steel grade was employed (Ike *et al.,* 2018).

Sachithanadam and Joshi (2016) stated that aspect ratio is fibre length to fibre diameter, so it can be said in relation to steel that Aspect Ratio is length of steel to diameter of steel. This length has influence on the steel which may be either by compression or tension. Research has consequently been directed toward reduction of materials resulting from corrosion in engineering application most especially in the pipeline industry.

As a result of weld failure or sour service environment cause about 60% of oil pipeline failure and 51% of natural gas pipeline, hence weld failure are considered the main stress raisers in a pipeline (Idokoh, 2016). During service, due to the nature of stress concentration, cracks can initiate in welded areas which are potential spots for crack initiation and subsequent propagation to sudden failure or collapse. As such effect of artificial crack aspect ratio on tensile and compressive properties on both weld and plain API X70 steel usually used in the transportation of oil and gas is studied to get insight on maintenance, repair and replace of materials used in the pipeline industries.

1.2   Statement of the Research Problem

As the world demand for energy increases by day, for thousands of years pipeline have been employed in the oil and gas industry which need and extent increases. But however, the oil and gas sector have continued to record huge economic losses due to pipeline failures, in terms of ruptures, explosion, leaks and spillage. This became necessary that we understand what causes such losses and how to improve the pipeline steels to curtail the losses. Many reports and research have pointed at weldment. In this research effort will be made to understand the effect of artificial crack aspect ratio on tensile and compressive properties of parent and welded API X70 steel. As such, information

regarding artificial crack aspect ratio may assist design Engineers in structural health monitoring, maintenance planning and replacement of structures if necessary.

1.3   Justification for the Study

Although, the current pipeline networks in Nigeria are still operational but it must be mentioned that they may have exceeded their design lives. As such some of the networks may require frequent inspection or replacement which would drive the need for higher steel grades such as the API X70 steel. Nigeria is blessed with crude oil and pipeline serve as the medium of transportation. Most structures have specified design life. It must be mentioned that most pipeline installation in Nigeria are made of the X55 and X60 grades which are lower in toughness compared to the recent grade such as X70, X80 and X100. Therefore, investigating the crack aspect ratio behaviour of X70 steel may provide information to pipeline Engineers towards future installations, maintenance and repairs.

1.4   Aim and Objectives of the Study

The aim of this research is to investigate the effect of artificial crack aspect ratio on tensile and compressive properties of welded API X70 steel. The aim will be achieved through the following objectives:

i.   To determine of the chemical composition of API X70 steel

ii. To determine tensile and compressive properties of plain and welded API X70 steel

iii. To determine effect of artificial crack aspect ratio on tensile and compressive properties of plain and welded API X70 steel.

1.5   Scope of the Study

API X70 steel was used in this research to determine the effect of artificial crack aspect ratio. Tensile and Compressive specimen were extracted from a round pipe which were milled to size required to carry out tensile and compressive test on them. The results obtained were used to estimate the effect of artificial crack aspect ratio on the steel. Tests were also supported by spectroscopic analysis and numerical analysis using ANYS 2019 R2.

CHAPTER TWO

2. 0   LITERATURE REVIEW

2.1   Theoretical Fundamentals

2.1.1   Introduction to literature review

This chapter presents literature reviews on mechanical properties of steels, grades of API

and failure in pipeline steel due to corrosion and its socio-economic damage remain

inevitable despite all the latest available techniques in combatting and protecting pipeline

steel against corrosion. Belmonte *et al.,* 2008 said pipeline service years in design is more

than 50 years and could exceed 100 years but fail long before this service life. Kolawole

et al., 2018 identified corrosion has been the biggest problem with API X70 steel pipeline

and other types of pipe in use in the oil and gas industry. Proper material selection has led

to the modern pipeline used in the oil and gas sectors today, although proper selection of

materials alone is not enough to combat corrosion in the steel pipeline (Kolawole *et al.,*

2018).

Degradation of pipelines is due mainly to the environment. This may lead to the reduction

in the integrity of material and potentially reduce the service life, causing premature

degradation or failure. Factors that may contribute or prevent the initiation and attack by

the environment are identified; such as pipe coatings, cathodic protection, soil conditions,

ambient conditions, temperature, stresses, pipe pressure and cyclic loading. In addition,

temperature and metallurgy variations can influence the material degradation. (Vesga,

2014)

Mechanical damage and corrosion are classified as two principal causes of the

deterioration of pipelines. The former could be caused by the manufacturing process, a

third party (welding, dent, gouges, spalling), soil settlement or movement (Llongueras *et*

al., 2005, Schmitt, 2006 and Dugsted, 2006). Also, residual stress, external stress and

secondary stresses are considered to reduce the service life of materials (Milne *et al.,* 1988). A review of API X70 steel and areas of application is first presented in the next section.

2.1.2 API X70 steel and areas of application

At about 30 years ago, high strength X70 grade steel with minimum 70.3ksi/483MPa yield strength was brought into the pipeline industry and its development was rapid with the introduction of thermomechanical (TM) rolling practices. Currently, pipeline materials in the world market are now being regulated according to the American Petroleum Institute's (API) standard 5L (Hillenbrand *et al.,* 1997). Hillenbrand *et al.,* 1997 observed that it is relevant to note that increasing the strength of structural steel offers the benefit of reduced steel weight/physical dimensions in terms of wall thickness and hence allows increased volume capacity

The chemical compositions of the X-grade steels are fairly simple, with maximum limits on C, Mn, S, P and other elements such as niobium and vanadium Ike *et al.,* 2018. The variations in strength (e.g., between X70 and X80) do not result primarily from variations in alloy composition, but from variations in the processing route of the steel Ike *et al*., 2018. Table 2.1 shows the chemical composition of API X70. However, a confirmatory test was carried out on the API X70 steel that was used for investigation in the present research. The result is discussed in chapter four.

Table 2.1: Chemical Composition of API X70 steel (%wt)

Steel	C	Mn	Si	P	S	Al	Nb	Cu	Cr	Ni	V	Ti
X70	0.08	1.604	0.31	0.019	0.005	0.023	0.03	0.013	0.138	0.012	0.046	0.01

Source: Natividad *et al.,* 2017

Offshore and gas exploration and production is mainly into water depth greater than 3000m, which are challenging to the well-established designs and pipe used (Natividad *et al.,* 2017).

In the early 1960s, in the pipeline industry medium carbon steel was the materials used but due to technological development in processes such as welding, use of micro alloying element in steel and thermomechanical control process (TMCP) high strength steel has been produced and even low carbon steels with high strength as well as weldability (Natividad *et al.,* 2017).

The current focus on less wall thickness at strength level leads to the development of API X80 and X100 grades (Natividad *et al.,* 2017). API X70 steel under different thermomechanical treatments exhibit different microstructure, texture and mechanical properties (Ike *et al.,* 2018). Figure 2.1 a relationship between stress and elongation of API X70 steel subjected to different heat treatment.
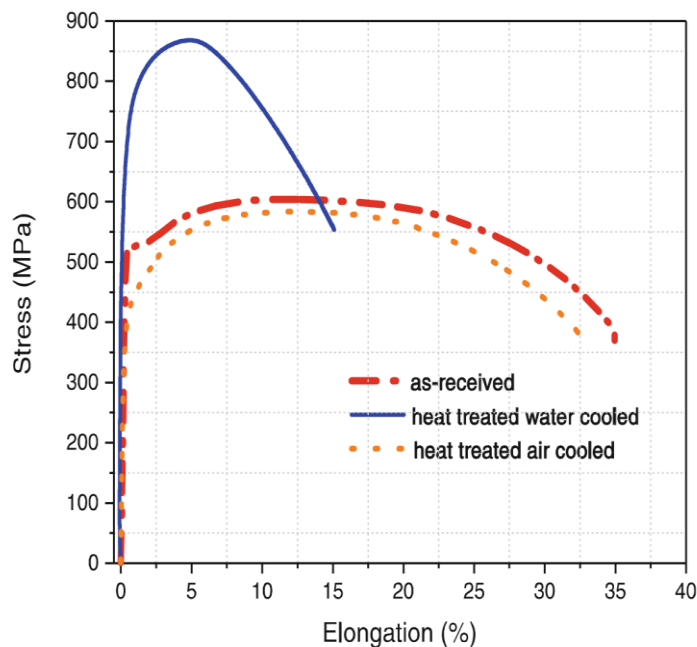
Figure 2.1: Stress-elongation for API X70 Steel (Source: Natividad *et al.,* 2017)

Figure 2.1 shows the stress-strain curve obtained from API X70 with and without heat treatment. The tensile properties and impact result of API X70 steel with or without heat treatment is summarized in table 2.2

Table 2.2: Tensile properties and Impact result of API X70 with or without Treatment

Steel (X70)	UTS (MPa)	YS (MPa)	$\sigma_{RUPTURE}$ (MPa)	EL (%)	EA (J)
As-received	604	522	350	35	176
Heat-treated water-cooled	868	644	550	15.2	60
Heat-treated air-cooled	584	512	375	34.7	130

Source: Natividad *et al.*, 2017

2.1.3   Grade of API steel

The development of modern pipeline steel has been performed in an effort to obtain an excellent combination of mechanical properties such as strength, toughness, ductility and weldability thus improving their performance to operate in harsh environments. High Strength Low Alloy Steels (HSLA) were developed for their potential to be used for high pressure requirements (>15 MPa) without increasing wall thickness but improving economic feasibility in the transportation of gas in arctic regions and in the exploitation of sour oil and gas reserves.

The most common HSLA steels in operation are made of API X52, X60, X65, X70, X80 and lately, X100 and X120 Vesga, 2014. In (Hillenbrand *et al.,* 1997), it was mentioned that pipeline materials are being used due to peculiar nature of mixed phase microstructures coupled with fine grain. It was also mentioned that the highest grade of pipeline steel that can be manufactured with pearlite-ferrite microstructure while retaining the weldability as well as ductile-brittle transition temperature is the X70 steel grade (Hillenbrand *et al.*, 1997). However, it could be said that the quest for better manufacturing techniques that will enhance toughness and other related mechanical

properties therefore informed the recent use of high strength low alloy steels (HSLA), which include X52, X60, X65, X70, X80, X100 and X120 (Vesga, 2014). Their reliable mechanical properties may be a factor that justifies their usage for structural applications as well as in the transportation of oil and gas products.

Farhad *et al.* (2017) revealed that with increase in pit aspect ratio and applied stress there is decrease in the local stress ratio after examining four different samples of API X65 steel under different pit geometry. Figure 2.2 and Table 2.3 clearly shows the trend of pit local stress ratio and pit aspect ratio. These study gives an insight that crack aspect ratio cannot be neglect in design consideration, fabrication and maintenance of pipeline steel.
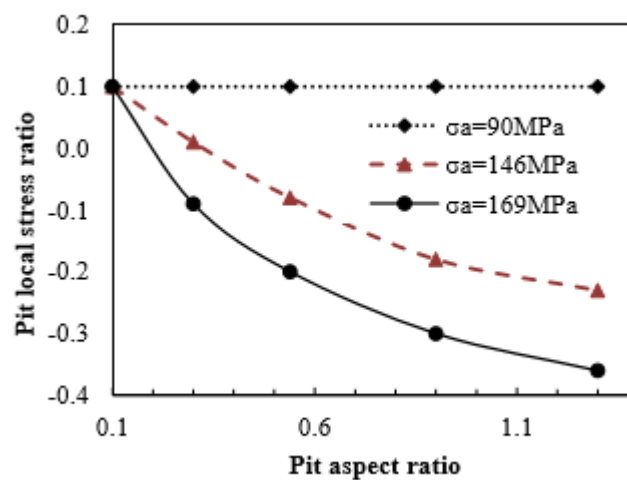
Figure 2.2: Relationship between local stress ratio and pit geometry with respect to applied stress. (Source: Farhad *et al.,* 2017)

Table 2.3: Pit Geometries Created on each Fatigue Tests Sample

Sample Number	Depth, a (mm)	Pit width, 2c	Aspect Ratio, a/2c
1	0.0763	0.6	0.13
2	**0.0851**	0.676	0.13
3	0.0344	0.271	0.13
4	0.0674	0.608	0.11

(Source: Farhad *et al.,* 2017)

2.1.4 Welding

Welding is one of the most important techniques in the fabrication industries to join metals in different geometries and sizes with cost-effective and reliable assembly. There are several types of welding processes used in the petrochemical industry that have been around for many decades and new methods developed in recent years. Basically, these processes vary in setup, essential variables and non-essential variables, such as shielded metal arc welding (SMAW), gas tungsten arc welding (GTAW), etc. Each welding process has characteristics that affect its quality performance and the soundness of the weld. For example, a weld acceptable for one application, such as for a tank, may not meet the acceptance criteria for pressure vessels per applicable international codes. Welding imperfections such as cracks, porosity, lack of fusion, incomplete penetration, and spatter could be due to various causes, such as poor workmanship, design issues, incorrect material, improper weld procedure specifications, and/or an unfavorable environment. The impact of each defect varies from acceptable to not acceptable, and must be either repaired or cut-out (Adedipe, 2015).

Therefore, it is important to ensure the quality and reliability of welds in equipment prior to placing it into service using nondestructive testing (NDT) methods and ensuring compliance with the requirements of international standards. Moreover, piping systems should be hydrotested to ensure the integrity and strength of the entire system. Some

welding defects, however, can only be discovered while the facility is in operation, such as crack initiation. These defects will require engineering assessment, such as Fitness-for-Service, to determine the proper remedial action.

2.1.5 Analysis of pipeline welding defect

Manufacturing processes have a large impact on the final outcome of a steel pipeline material in terms of its material properties. The degree of variability in material properties within finished pipe has been observed as a function of rolling practices and the new compositions which are incorporated into the process (Smart and Bond, 2016). Figure 2.3 grouped weld defects into external and internal defects
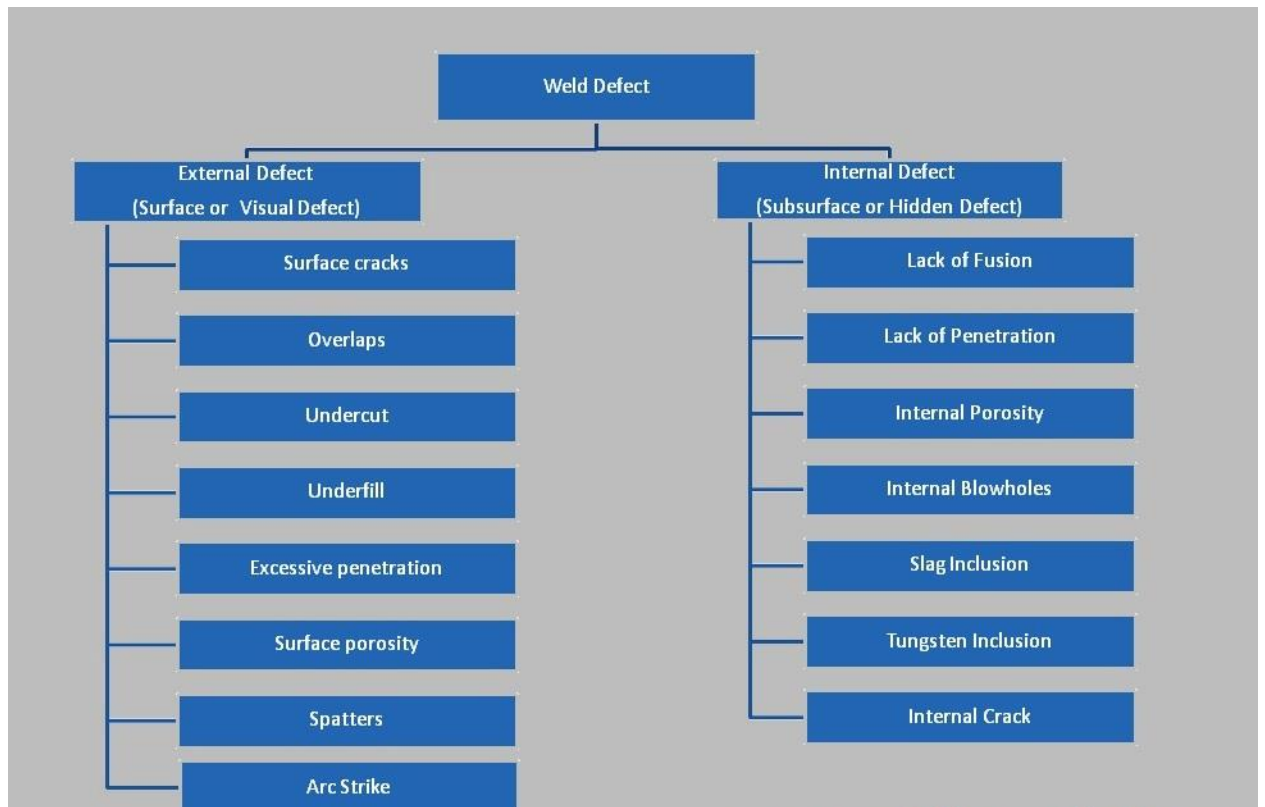
Figure 2.3: Different kind of weld defects
Source: (Anand, 2017)

2.1.5.1 Crack

The crack occurs when localized stress exceeds the ultimate Tensile Stress (UTS) of the material. It may propagate within the material. Cracks appear anywhere, can be surface, subsurface, depth or root. Its either microscopic or macroscopic, any size or shape. It is considered the most dangerous of all defects. (Anand, 2017). Figure 2.4 gives a pictorial diagram of crack on a weld metal after undergoing dye penetration.

Figure 2.4: Cracks observed during dye penetration test.
Source: (Anand, 2017)

Anand (2021) in his blog further divided cracks into two types; which are hot and cold crack. Hot crack usually occurs during solidification of the molten weld pool, it occurs in the weld metal (Solidification Crack) and it can also occur at the Heat Affected Zone (HAZ) region (Liquation Crack). Crack defaults in weld are usually caused by rapid cooling of the molten weld pool, poor ductility of the welding materials, high concentration of residual stresses, inadequate heat treatment which can be readily prevented by using filler metal while welding and carrying out pre heating and post heating to avoid rapid cooling.

Cold cracks can develop several days after welding. It occurs after solidification of the weld metal. Most of the time it develops in the HAZ but may occur on the weld metal too. It is often associated with non-metallic inclusion. Diffusion of Hydrogen atoms and

lack of pre heating usually cause cold cracks which can be prevented preheating and post welding the weld metal and use of low hydrogen electrode (Anand, 2017).

2.1.5.2 Porosity

Porosity is the result of gas being entrapped in solidifying weld metal and is generally spherical but may be elongated. Uniformly scattered porosity may be scattered throughout single weld passes or throughout several passes of a multipass weld. Faulty welding technique or defective materials and poor weld hygiene generally cause porosity. Anand (2021) blogged that cluster porosity is a localized grouping of pores that can result from improper arc initiation or termination. Linear porosity maybe aligned along a weld interface or root or between beads. It is caused by contamination along the boundary. Piping porosity is elongated and, if exposed to the surface, indicates the presence of severe internal porosity. Porosity has little effect on strength, some effect on ductility, and a significant effect on fatigue strength and toughness. External porosity is more injurious than internal porosity because of the stress concentration effects.

Porosity is considered a spherical and nonplanar imperfection and therefore is not a serious threat to weld in normal loading and even in fatigue conditions. The tolerance of porosity in such conditions is much more liberal, and often up to 5% porosity in a standard radiograph length is accepted. However, if the weld that is required to have good toughness to resist brittle fracture at lower temperatures, especially when the Charpy impact values of weld metal is required 40 J (30 ft-lb) or higher, the porosity is treated as a planar imperfection.

2.1.5.3 Inclusions

Slag inclusions are nonmetallic particles trapped in the weld metal or at the weld interface. Slag inclusions result from faulty welding technique, improper access to the joint, or both. Sharp notches in joint boundaries or between weld passes promote slag entrapment. With

proper technique, slag inclusions rise to the surface of the molten weld metal. Basically, there are four types of inclusions: Tungsten inclusion, Oxide inclusion, Slag inclusion and Flux inclusion. Tungsten inclusions are tungsten particles trapped in weld metal deposited with the gas tungsten arc welding process. Dipping the tungsten electrode in the molten weld metal or using too high current that melts the tungsten can cause inclusions. (Anand, 2017). Figure 2.5 has three dots in the red region these depicts inclusion in the weldment.
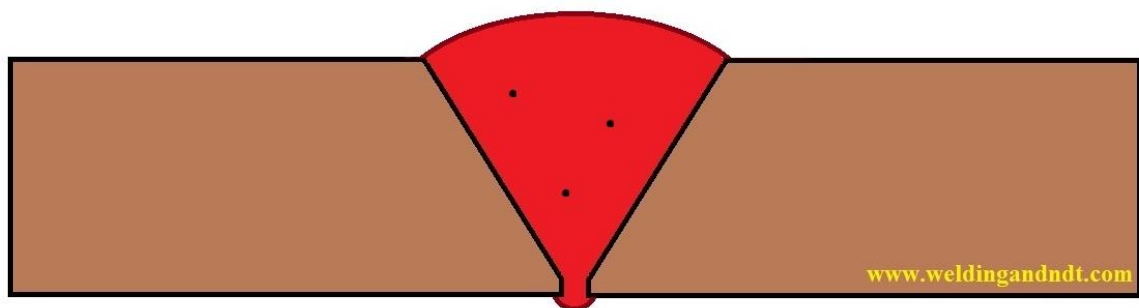
Figure 2.5: Inclusions in weldment.
Source: (Anand, 2017)

2.1.5.4 Incomplete fusion

Incomplete Fusion also known as cold lapping or cold shut is the lack of proper melting (or proper fusion) either between the weld metal with the base metal or one layer of the weld with the other layer. Incorrect welding techniques, improper preparations of materials, or wrong joint designs promote incomplete fusion in welds. Insufficient welding current, lack of access to all faces of the joint, and insufficient weld joint cleaning are additional causes. This is a stress-concentrating flaw and can in most cases initiate cracks. Figure 2.6 pictures lack of fusion between the base metal and weld metal.
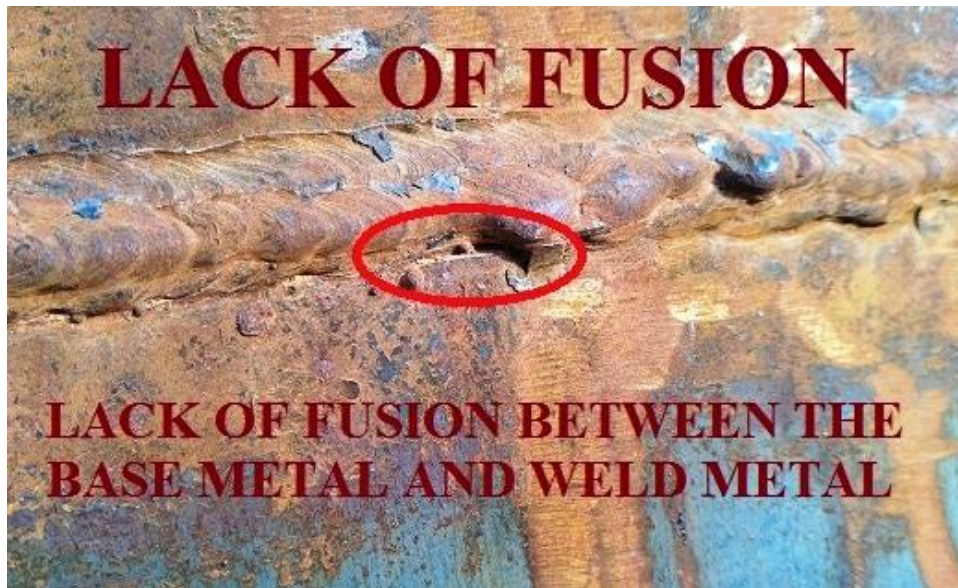
Figure 2.6: Incomplete Fusion between Base Metal and Weld Metal (Anand, 2017)

2.1.5.5 Inadequate joint penetration

When the actual root penetration of a weld is less than specified, the discontinuity at the root is called inadequate penetration. This may result from insufficient heat input, improper joint design (metal section too thick), incorrect bevel angle, or poor control of the arc. Some welding procedures for double groove welds require back gouging of the root of the first weld to expose sound metal before depositing the first pass on the second side to ensure that there is not inadequate joint penetration. Similar to incomplete fusion discussed earlier, incomplete penetration is a stress-concentration point, and cracks can initiate in the unfused area and propagate as successive beads are deposited. Cyclic loading can initiate catastrophic failures from incomplete penetration (Anand, 2017).

Figure 2.7: Inadequate Joint Penetration
Source: (Anand, 2017)

2.1.5.6 Surface irregularities

Surface pores are caused by improper welding technique such as excessive current, inadequate shielding, or incorrect polarity. They can result in slag entrapment during subsequent welding passes. Variations in weld surface layers, depressions, variations in weld height or reinforcement, no uniformity of weld ripples, and other surface irregularities can indicate that improper welding procedures were followed or that welding technique was poor. (Adedipe, 2015)

2.1.6   Tensile test

The mechanical properties of materials are determined by performing designed laboratory experiments that replicate as nearly as possible the service conditions. In the real life, there are many factors involved in the nature in which loads are applied on a material. The following are some common examples of how these loads might be applied: tensile, compressive and shear, just to name a few. These properties are important in materials selections for mechanical design. Other factors that often complicate the design process include temperature and time factors.

The results of tensile tests are used in selecting materials for engineering applications. Tensile properties frequently are included in material specifications to ensure quality.

Tensile properties often are measured during development of new materials and processes, so that different materials and processes can be compared. Finally, tensile properties often are used to predict the behavior of a material under forms of loading other than uniaxial tension.

The strength of a material often is the primary concern. The strength of interest may be measured in terms of either the stress necessary to cause appreciable plastic deformation or the maximum stress that the material can withstand. These measures of strength are used, with appropriate caution (in the form of safety factors), in engineering design. Also of interest is the material's ductility, which is a measure of how much it can be deformed before it fractures. Rarely is ductility incorporated directly in design; rather, it is included in material specifications to ensure quality and toughness. Low ductility in a tensile test often is accompanied by low resistance to fracture under other forms of loading. Elastic properties also may be of interest, but special techniques must be used to measure these properties during tensile testing, and more accurate measurements can be made by ultrasonic techniques. (ASM International, 2014)

2.1.6.1 Tensile specimens and testing machines

a. Tensile specimens

Consider the typical tensile specimen shown in Figure 2.8. It has enlarged ends or shoulders for gripping. The important part of the specimen is the gage section. The cross-sectional area of the gauge section is reduced relative to that of the remainder of the specimen so that deformation and failure will be localized in this region. The gauge length is the region over which measurements are made and is centered within the reduced section. To avoid end effects from the shoulders, the length of the transition region should be at least as great as the diameter, and the total length of the reduced section should be at least four times the diameter.
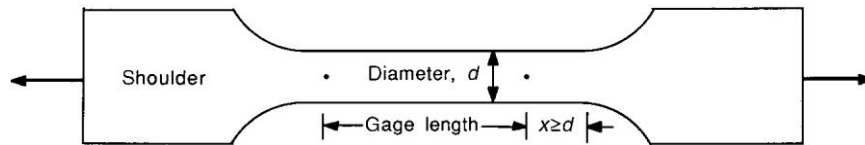
Figure 2.8: Typical tensile specimen, showing a reduced gage section and enlarged shoulders. (ASM International, 2014)

b.   Testing machines

The most common testing machines are universal testers, which test materials in tension, compression, or bending. Their primary function is to create the stress strain curve. Testing machines are either electromechanical or hydraulic. The principal difference is the method by which the load is applied. Electromechanical machines are based on a variable-speed electric motor; a gear reduction system; and one, two, or four screws that move the crosshead up or down. This motion loads the specimen in tension or compression.

c.   Stress-strain curves

A tensile test involves mounting the specimen in a machine, such as those described in the previous section, and subjecting it to tension. The tensile force is recorded as a function of the increase in gage length. Engineering stress, or nominal stress, s, is defined as:

$$s = F/A_0 \hspace{5cm} 2.1$$

where F is the tensile force and A_0 is the initial cross-sectional area of the gage section. strain, or Engineering nominal strain, e, is defined as: (ASMI, 2014)

$$e = DL/L_0$$

where L_0 is the initial gage length and DL is the change in gauge length (L-L_0).

When force-elongation data are converted to engineering stress and strain, a stress-strain curve that is identical in shape to the force-elongation curve can be plotted. The advantage

of dealing with stress versus strain rather than load versus elongation is that the stress-strain curve is virtually independent of specimen dimensions.

d.   Elastic versus Plastic Deformation

When a solid material is subjected to small stresses, the bonds between the atoms are stretched. When the stress is removed, the bonds relax and the material returns to its original shape. This reversible deformation is called elastic deformation. (The deformation of a rubber band is entirely elastic). At higher stresses, planes of atoms slide over one another. This deformation, which is not recovered when the stress is removed, is termed plastic deformation.

2.1.7   Compression test

When a material is subjected to compressive loading, the relationship between stress and strain is similar to that obtained for a tensile loading. Up to a certain value of stress, the material behaves elastically, that is stress is in proportion to strain. Beyond this value, plastic flow starts, that is more strain starts than happening in elastic limit for any increment value of loading. It is seen that a compression test is more difficult to be conducted than standard tensile test due to: (ASMI, 2014)

(i)   specimen must have larger cross-sectional area to resist any buckling due to bending,

(ii)   The specimen undergoing strain hardening as deformation proceeds, and

(iii)   Cross-section of the specimen increases with deformation, thereby requiring substantial increase in the required load.

The lateral instability due to buckling action can be avoided by keeping the ratio of height (h) to diameter (d) of the specimen less than 2. The compressive strength essentially depends open 'h' to 'd' ratio. Hence, higher is 'h' to 'd' ratio, lower is the

compressive strength. All this was put into due consideration when preparing the samples for compression test.

2.2 Review of Related Literature

2.2.1 Microstructure and mechanical relations

Since microstructure is a key variable in determining material properties, it must be specifically designed to ensure safe and optimal performance under operating conditions (Stalheim and Muralidharan, 2006). Most modern line pipe steels have different and complex microstructural arrangements depending on their chemical compositions and processing routes {that is thermomechanical control process (TMCP) plus accelerated cooling condition (ACC)}. However, prevails a general tendency to reduce carbon content in industrial 'conventional' plates

The appropriate chemical composition, rolling temperature, finish temperature, cooling rate and cooling interrupted temperature are the most significant variables that affect the final microstructure and have been studied extensively (Barsanti *et al.,* 2002, Hillenbrand *et al.,* 2008 and Zhao *et al.,* 2003). Zhuang *et al.,* 2012 studied the microstructure and mechanical properties of low carbon steel under different processing and cooling parameters. They stated that the austenite cannot be recrystallized or only partially recrystallized within or after deformation at relatively low deformation temperature and short inter-pass time which induced the deformation induced ferrite transformation (DIFT).

From the TMCP process, different microstructures can be obtained which are classified into four types: polygonal ferrite (P-F), quasi-polygonal ferrite (Q-F), granular bainite-ferrite (GB-F) and bainite-ferrite (B-F). P-F is transformed at the highest temperatures and slowest cooling rates which nucleate as grain boundary allotriomorphs growing into equiaxed grains (Gray, 1974).

Q-F and its austenite parent can be transformed together in grains with irregular boundaries containing a high density of dislocations and martensite/austenite (M/A) islands. B-F consists of an elongated ferritic lath with a high density of dislocations and is separated by low angle grain boundaries (LAGBs). G-F is obtained by slower cooling rates containing a high density of dislocations and is separated by LAGBs (Wang *et al.,* 2009).

The effect of TMCP on the microstructure of HSLA steel was investigated by Zhao *et al.,* 2003. They found that the acicular ferrite (A-F) dominated the microstructure and as a result strength and toughness were enhanced. A similar study was made on a commercial API X70 grade P-F microstructure and X90 grade A-F microstructure by Wang *et al*., 2009. It was found that strength and toughness are similarly improved; however, the elongation and Y/T ratio of both steels were not changed by the thermal treatment. A high density of dislocations was observed. Hillenbrand et al. carried out studies on the impact of microstructures on the mechanical properties of X70, X80 and X100 pipeline steels. Their investigation concluded that strength and toughness were increased by modifying the microstructure from Pearlite-Ferrite (P-F) to Ferrite-Bainite (F-B), leading to the development of the X80 grade. Examples of this microstructure of HSLA steels can be seen in Figure 2.9. The X70 matrix corresponds to F-P, X80 is compound of F-B and X100 by bainite. However, characterization of this structure, mainly X80 and beyond is restricted under optical microscopy.
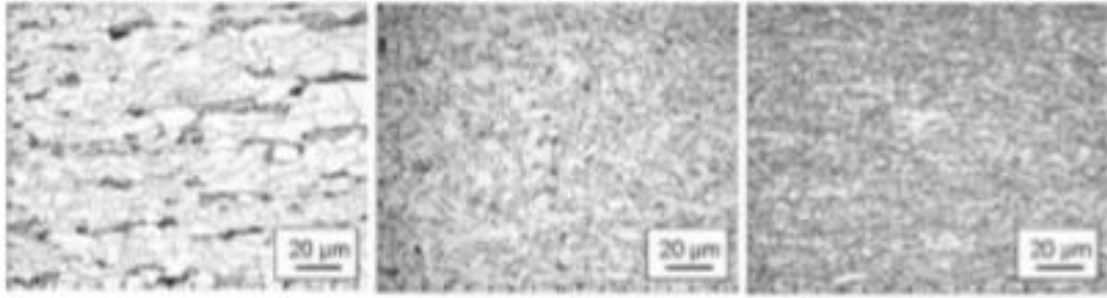
Figure 2.9: Microstructure of HSLA pipeline steels: X70 (left), X80 (centre), X100 (right) (Hillenbrand *et al.,* 2008)

Electron microscopy combined with electron backscatter diffraction (EBSD) has been demonstrated to be powerful. Characterizations of the micro texture, measure of the grain size, type of bainite and crystal orientation allow a more precise identification of the category of steel.

2.2.2 Effect temperature

It has been argued in the literature (Vesga., 2014) that fracture properties are reduced as temperature reduces and thus causing a brittle fracture failure mechanism. Temperature contributes significantly to fracture properties of pipelines steels. The effect of temperature on fracture properties of API X65 pipeline steel was also carried out by (Nonn and Brauer 2014) at temperatures of -20 °C -60 °C, -80 °C, -100 °C and -120 °C respectively. Results also showed a significant effect of temperature on charpy V-notch energy values as there was a drop in the values from 216J at -20 °C to 16J at -120 °C for 10 mm thick specimens. As mentioned, the set back of most of the investigations that are discussed in this section as well as in previous sections is that fracture properties of weld pipeline steels have not been adequately investigated.

2.2.3 Effect of crack aspect ratio

For many engineering components and structures, short fatigue crack behaviour controls the majority of total fatigue life. A number of researchers have reported that these short cracks propagate much faster than long cracks under equivalent stress intensity factor ranges Temerature change (ΔK) (Miller, 1982; Taylor and Knott, 1981 and Hudak, 1981). Conventionally, small crack data analysis approaches employ secant or polynomial data reduction, assuming that small crack shapes are semi-circular i.e ratio of area to depth equal to 1 (a/c=1). However, the results of Ravichandran's study (Ravichandran and Larsen, 1997, Ravichandran, 1997) strongly indicate that some of these apparent characteristics of small cracks, often referred to as anomalous, are in fact partly due to the assumption that a/c=1. With this in view, in this study the aspect ratio ranges from 0.2 to 1 was employed (a/c rages 0.2 - 1).

In plates with a surface crack under tension loading, the maximum Stress Intensity Factor (SIF) is reached at the crack center when the aspect ratio is lower than 0.6 and at the border when it is higher (Newman and Raju 1979). For embedded cracks, the maximum SIF is achieved near the free surface (Guozhong *et al.,* 1996). In the case of corner cracks, the highest values of the SIF occurred at the free surface along the width direction for cracks in which the depth is higher than the other dimension and at the free surface along the thickness direction for cracks in which the depth is lower than the other dimension (Raju and Newman, 1987). The existence of free surfaces has a great influence on crack advancement. Cracks tend to propagate reaching a constant SIF along their front (iso-K), but the free surface prevents this phenomenon (Lin and Smith, 1999).

Qin *et al.,* 2018 carried out research on the effect of area, aspect ratio and orientation of rectangular nanohole on the tensile strength of defective graphene, from the study it was

discovered that the tensile strength of defective graphene is more sensitive to the tilting angle of nanoholes at larger areas and aspect ratio than smaller areas and aspect ratio. These findings provide useful guidelines for designing the specimens for the research.

In previous work (Yap *et al.,* 2016), on the effect of aspect ratio and volume fraction on mechanical properties of steel fibre-reinforced oil palm shell concrete form the result obtained, that the highest compressive strength of 47 MPa with aspect ratio of 65. It was concluded that the compressive strength of oil palm shell reinforced concrete depends on the aspect ratio. Effect of aspect ratio on modulus of elasticity was also observed in the study, the higher the aspect ratio, the lower the modulus of elasticity (Alengaram *et al.,* 2011a).

Barsanti *et al.,* 2002 carried out an experiment on the effect of aspect ratio and volume fraction of steel fibers in strength properties of geopolymer concrete. Steel fiber of different aspect ratio was used and the test results point out that adding up of hook end steel fibers improves compressive strength at all the ages. The increase in aspect ratio of hook end steel fibers increases the compressive strength of GPC. When a split tensile test was also performed the result also revealed an augmented increased in tensile strength as the aspect ratio increases. This result obtained by Barsanti *et al.,* 2002 is also similar to the result obtained by Yap *et al.,* 2016.

2.3   Research Gap

Ravichandran and Larsen, 1997 did carried out research on the effects of crack aspect ratio on the behavior of small surface cracks in fatigue on a Titanium alloy using one aspect ratio of 1.0 but in this research five different aspect ratio was observed and with conditions varied for both length and depth, which gives it a broader view of the bahaviour of crack aspect ratio on materials. For Baskar *et al.,* 2019 steel fibres of

different aspect ratios were considered for both compressive and tensile test the result obtained were in agreement with Yap *et al.,* 2016 but welded steel materials were not considered.

CHAPTER THREE

3.0   **MATERIALS AND METHODS**

3.1   **Materials**

The materials and equipment used for this research are:

1. Parent Material API X70 welded and unwelded steel

2. Tensile Machine

3. Compression Machine

4. Hack saw

5. Acetylene and Oxygen gas (For cutting sample from the parent material)

6. Milling Machine

7. ANSYS 2019 R2

8. Optical microscope

9. Spectroscopic analysis machine

3.2 Methods

3.2.1 Sample preparation

API X70 pipeline steel plates of thickness 20.8 mm with equal width and length (304.8 mm) was used as the base metal or test specimen. This material was obtained from the engineering. Laboratory of the Pipe Construction Factory belonging to Shabiv Construction Company (SCC)

Nig Ltd at Ushafa, Bwari, Abuja FCT. It was cut from the base pipe (Plate I) using acetylene and oxygen gas, then further taking to the laboratory where milling machine (plate Ib) was employed to shape it into the desired shape (plate III a, b, c and d) for tensile and compressive test. A total of 30 samples each of both weld and plain samples were produced for tensile test and compression test. Plate IVa and b shows artificial

defects were made in these samples in form of aspect ratio using drill machine of different

bit to inscribe defects of different aspect ratio on both the plain and weld samples.

Plate I: Pipe were the parent API X70 was cut.

Plate IIa: Universal Testing Machine

Plate IIb: Milling Machine

Plate IIIa: Prepared Plain Tensile Sample

Plate IIIb: Prepared Weld Tensile Sample

Plate IIIc. Prepared Plain Compression Sample

Plate IIId. Prepared Weld Compression Sample

Plate IVa. Prepared Plain Tensile Samples with Artificial Defects

Plate IVb. Prepared Weld Tensile Samples with Artificial Defects

3.2.2 Experiment

The method used for this research is subdivided into two categories; analysis of the specimen and destructive test evaluation using the universal testing machine at Kaduna State Polytechnic Civil Engineering Laboratory. A simulation test was run using ANSYS 2019 R2. The most common shape factor is the aspect ratio; it is a ratio of crack length to crack depth of a defect. Aspect ratio is described in equation 1 and it is schematically shown in figure 3.1.

$$Aspect\ ratio = \frac{a}{c} \hspace{4cm} 3.1$$
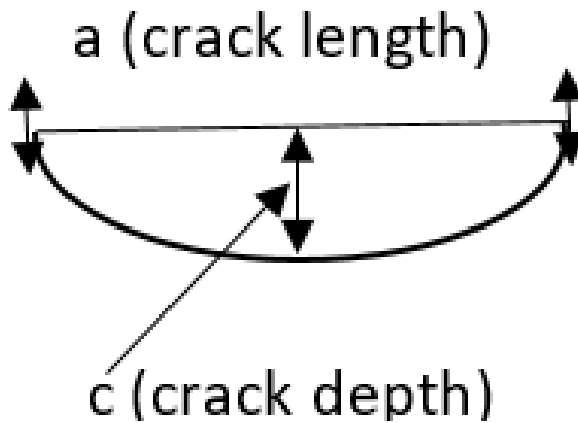
Figure 3.1: Schematic representation of aspect ratio

Five different lengths and depths were considered in creating the artificial surface defects on both the plain and the weld API X70 steel, 5mm, 4mm, 3mm, 2mm and 1mm dies were used to create the defects.

3.2.3 Chemical analysis

The chemical composition of the base metal plate being used (API X70) was obtained by conducting a chemical analysis in the laboratory in Ushafa, Bwari FCT Abuja. The result obtained is set out in the discussion section.

3.3.3 Tensile test

Tensile specimens of the base metal were produced with and without artificial surface defects. Similarly, weld samples were also produced with and without artificial surface defects. Depth and Length were varied for both plain and weld specimens with surface defects representing aspect ratio. The schematic diagram of the tensile test specimen designed according to ASTM D638 (ASTM D638, 2013) is shown in Figure 3.2a and b.
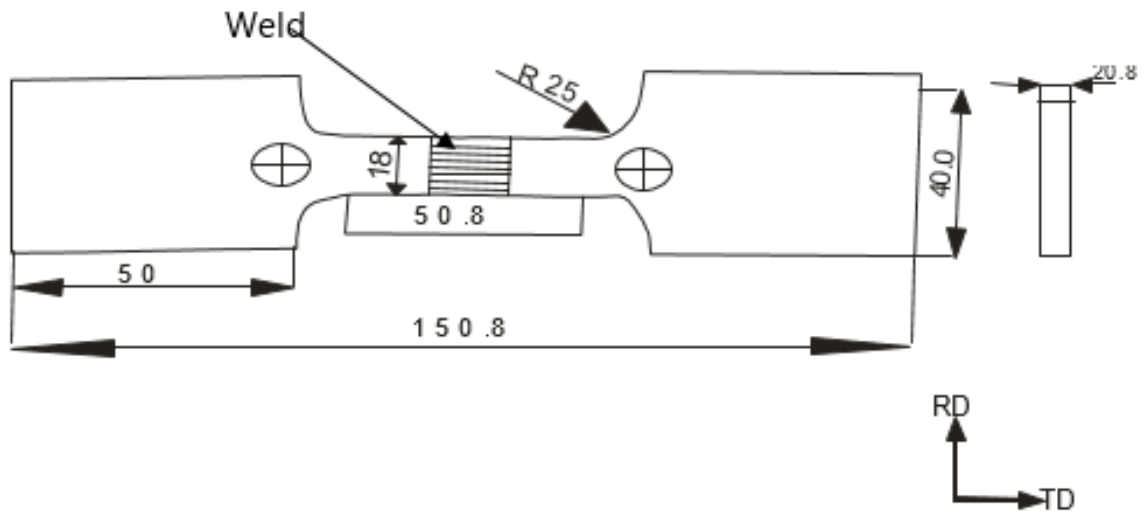
Figure 3.2a: Tensile test specimen design
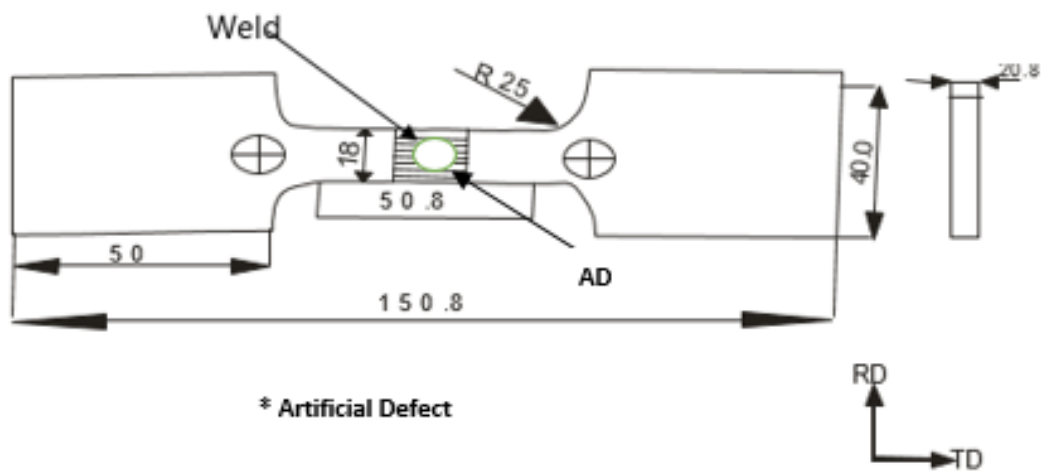
Figure 3.2b: Tensile test specimen with artificial defect design

3.3.3 Compression test

Compression specimens of the base metal and weld materials were produced with and without artificial surface defects. Depth and Length were varied for both plain and weld specimens with surface defects representing aspect ratio. In all, a total of thirty specimens for compression test were produced for testing. The schematic diagram of the compression test specimen designed according to ASTM D638 is shown in Figure 3.3a and b.
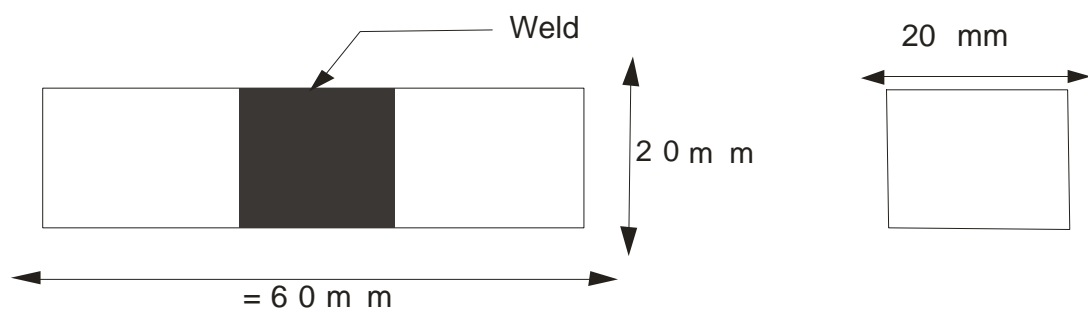
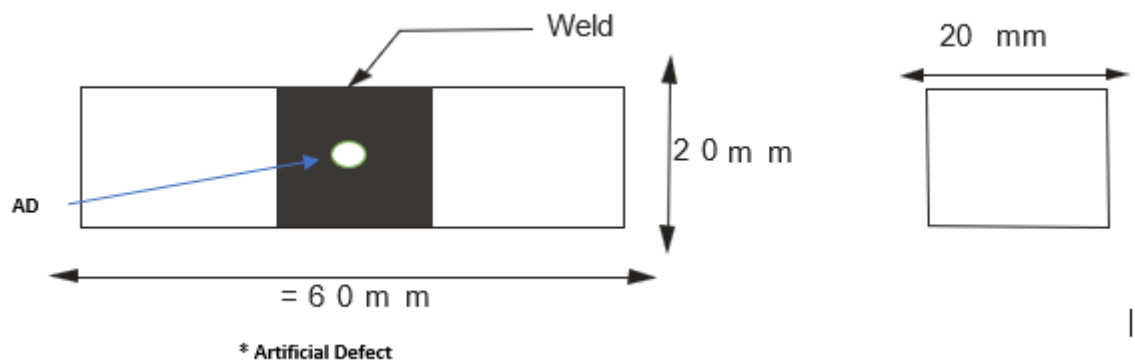

Figure 3.3a: Compression test specimen design

Figure 3.3b: Compression test specimen with artificial defect design

CHAPTER FOUR

4.0   **RESULTS AND DISCUSSION**

4.1   Chemical Analysis Result

The result obtained from the chemical analysis conducted on the API X70 steel is tabulated in Table 4.1. The essence of this analysis was to establish the material conformity with the chemical analysis that was presented in a previous study as shown in Table 4.2 (Ike *et al.,* 2019).

Table 4.1: Chemical composition of API X 70 steel

Element	%C	%Si	%S	%P	%Mn	%Cr	%Mo	%Ni	%V	%Cu	%Al	%Co	%Pb
Actual	0.051	0.210	<0.003	<0.005	1.500	0.239	0.118	0.017	0.012	<0.002	0.048	0.086	<0.003

The result of chemical analysis was in agreement when compared with those obtained in Ike et al., 2019. The chemical composition for the most common elements in steel as reported by Ike et al., 2019 were 0.051%C, 0.210%Si, <0.003%S, <0.005%P, 1.500%Mn and 0.24%Cr; and these values are in close agreement with the ones obtained in this research. The variation of some of the elements may be as a result of experimental condition. The result was also compared with those reported in literature for the same material (Leonardo *et al.,* 2014; Vesga, 2014*).* Leonardo et al. work compare well with the results presented in Table 4.1, especially for manganese which was 1.536% (Leonardo *et al.,* 2014) and 1.89% (Vesga, 2014) as against 1.50% in the present study. The carbon content was also found to be within the same range. Comparing the chemical analysis results of the steel used in this research with those published in the literature, it appears that the steel satisfies the API requirements.

4.2 Effect of Aspect Ratio on Tensile and Compressive Properties of API X70

4.2.1 Tensile test results and discussion

Figure 4.1 shows the several tensile samples for both welded and parent materials subject to tensile test using the universal testing machine. Specimen A is a weld with an artificial aspect ratio of 1mm, showing no necking but failed at the point where the artificial aspect ratio was made, while specimen B is a weld metal without artificial defects, necking occurred at the gauge. Specimen C and D are both plain with artificial aspect ratio of 0.2 and plain parent metal without artificial aspect ratio. It was observed that for the weld with artificial aspect ratio did not experience necking while small necking was observed on a plain material specimen.

Figure 4.1: Weld and Parent Specimen subjected to destructive test (Tensile Test)

The maximum stress obtained for plain material without defect was 706.8 MPa while for specimens with defects, the maximum stress for an aspect ratio of 0.2 was obtained to be

709.8 MPa. However, for plain material with defect the lowest value of maximum stress was obtained at an aspect ratio of 1.0 to be 646.8 MPa. This implies that for tensile specimens, the lower the aspect ratio, the higher the stress. For weld material without defect, the maximum stress obtained was 667.8 MPa, while for weld material with defect, the maximum stress was obtained to be 688.8 MPa at aspect ratios of 0.2. The lowest value of the maximum stress for weld tensile specimen was obtained to be 643.3 MPa at an aspect ratio of 1. It can be observed that the higher the aspect ratio, the lower the stress while it is the other way round when compared to plain tensile specimens. Sharma and Maheshwari (2017) also stated that the microstructure of welds is determined by the chemical composition of the parent material, heat applied during welding and the chemical composition of the filler materials. Therefore, the weld results may have been influenced by these aforementioned factors.
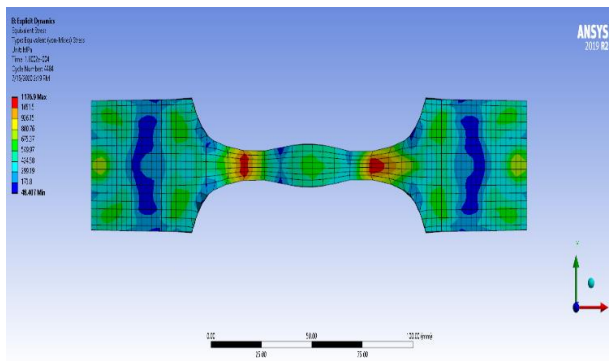
(a)
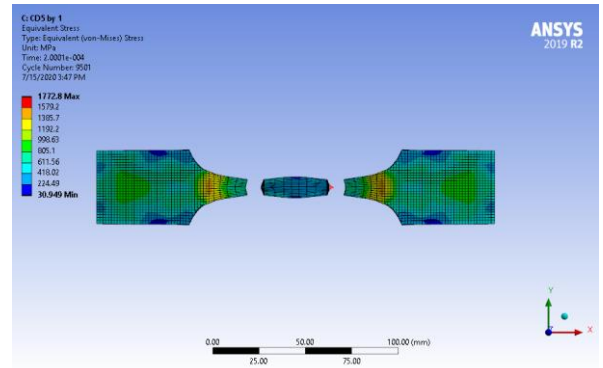
(b)
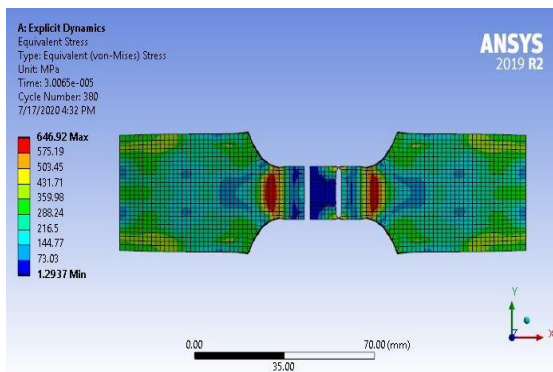
(c)
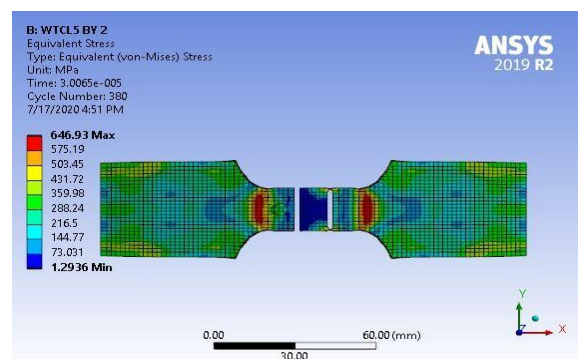
(d)

Figure 4.2: Tensile test result for (a) plain material, (b) Plain material with defect, (c) weld material, (d) weld material with defect using ANSYS 2019 R2

Table 4.2 presents aspect ratio and maximum stresses for both plain and weld with artificial crack. Similarly, it was observed that the maximum stress reduces as the aspect ratio increases for the plain materials with crack has a similar trend in weld materials.

Table 4.2: Result of Aspect Ratio and Maximum Stresses for Plain and Weld Tensile Specimen with Artificial Crack

Aspect Ratio	Maximum Stresses (Mpa)			
	Plain Material (MPa)		Weld material (MPa)	
	Constant Depth=5 mm	Constant Length=5 mm	Constant Depth=5 mm	Constant Length=5 mm
0.2	709.8	664.3	688.8	660.8
0.4	708.0	657.3	685.3	657.3
0.6	706.3	650.3	685.3	646.9
0.8	703.1	650.3	678.3	646.9
1	699.3	646.8	678.3	643.3

The result obtained for the plain tensile value gotten numerically using ANSYS 2019 R2 somewhat agree with the one obtained experimentally using the universal testing machine. Except for that of the welded material with defects which aspect ratio tends to have no significant effect. Table 4.3 show the result of the numerical value obtained

Table 4.3: Result of Aspect Ratio and Maximum Stresses for Plain and Weld Tensile Specimen with Artificial Surface Defects Numerical Value using ANSYS 2019 R2

Aspect Ratio	Maximum Stresses (Mpa)			
	Plain Material (MPa)		Weld material (MPa)	
	Constant Depth=5 mm	Constant Length=5 mm	Constant Depth=5 mm	Constant Length=5 mm
0.2	1772.8	1246.9	569.79	646.92
0.4	1578.1	1417	646.08	646.92
0.6	1534.8	1442.2	646.92	646.93
0.8	1219.9	1534.8	646.92	646.93
1	1124.6	1553.9	646.92	646.93

These results when compared with the results obtained using similar materials in the literature (Shin *et al.,* 2009; Leonardo *et al.,* 2014; Ike *et al.,* 2019) revealed good agreement. . However, in Ike *et al.,* 2019, the mean yield and tensile strenghts were 573.05 MPa and 651.57 MPa respectively. It can be seen that these results are close to those obtained form this present study which is 709.8 MPa and 688.8 MPa.

4.2.2 Compression test results and discussion

The Universal Testing machine was employed as discussed in chapter 3 to carry out the compression test. Compressive stress which is the reverse of tensile stress, Table 4.3 shows the result obtained for the compressive test carried out on Twenty different samples which are in Four different categories as started in chapter three.

The maximum stress obtained in plain and weld material without defect were 1200.4 MPa and 1300.2 MPa respectively. For the plain and weld materials with defect, the maximum

stresses were obtained to be 1238.5 MPa and 1500.5 MPa at aspect ratios of 1.0 and 0.2 respectively.

Table 4.4: Result of Aspect Ratio and Maximum Stresses for Plain and Weld Compression Specimen with Artificial Surface Defects

Aspect Ratio	Maximum Stresses (MPa)			
	Plain Material		Weld Material	
	Constant Depth=5 mm	Constant Length=5 mm	Constant Depth=5 mm	Constant Length=5 mm
0.2	1203.4	1101.3	1500.5	1475.5
0.4	1212.2	1103.6	1470.7	1456.6
0.6	1230.4	1109.7	1435.2	1445.4
0.8	1232.3	1117.8	1336.9	1389.7
1.0	1238.5	1127.7	1257.2	1259.8

The result show in table 4.4 agrees with the trend of result obtained from the simulation using ANSYS 2019 R2 whose result and figure is shown in Table 4.5 and Figure 4.3

(a)

(b)
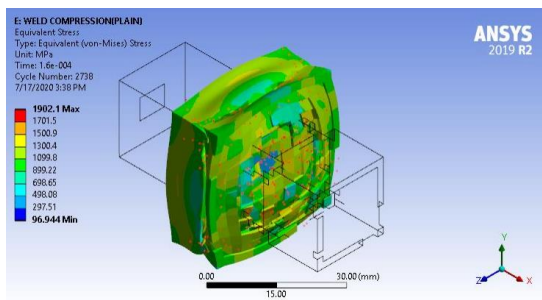
(b)
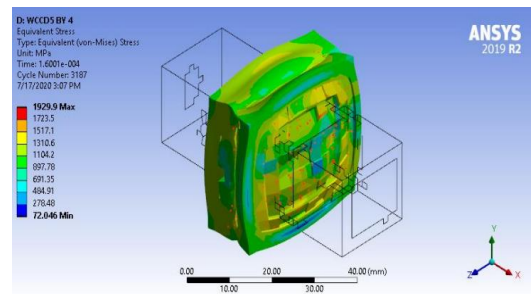
(c)

Figure 4.3: Compression test result for (a) plain material, (b) plain material with defect, (a) weld material, (b) weld material with defect

The results of compression tests carried out numerically by using the software ANSYS 2019 R2 on plain and weld materials wit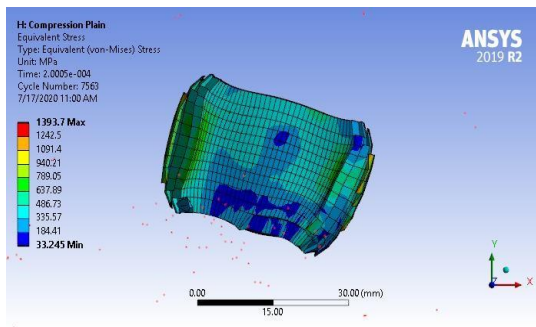h and without defects are shown in Table 4.5. The maximum stress obtained in plain and weld material without defect were 1393.7 MPa and 1902.1 MPa respectively. For the plain and weld materials with defect, the maximum stresses were obtained to be 1637.9 MPa and 1929.9 MPa at aspect ratios of 1.0 and 0.2 respectively.
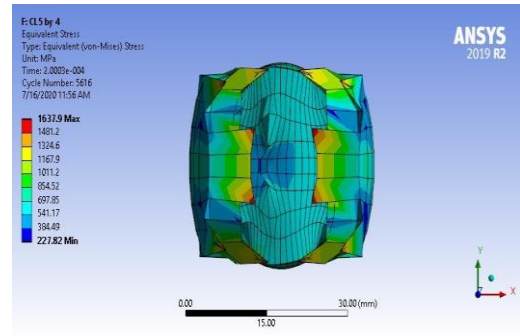
Table 4.5: Result of Aspect Ratio and Maximum Stresses for Plain and Weld compression specimen with Artificial Surface Defects Numerical Value using ANSYS 2019 R2

Aspect Ratio	Maximum Stresses (MPa)			
1	Plain Material		Weld Material	
	Constant Depth=5 mm	Constant Length=5 mm	Constant Depth=5 mm	Constant Length=5 mm
0.2	1614.3	1601.8	1929.9	1875.5
0.4	1621.0	1606.5	1875.5	1813.6
0.6	1627.6	1614.3	1830.4	1830.4
0.8	1631.2	1625.5	1782.4	1797.7
1.0	1637.9	1627.6	1688.8	1688.8

<center>**CHAPTER FIVE**</center>

5.0   **CONCLUSION AND RECOMMENDATIONS**

5.1   Conclusion

The effect of aspect ratio on tensile and compressive properties of API X70 steel was investigated for both plain and weld materials. The following conclusions can be drawn:

i.   API X70 steel base metal was observed to have better ductility owing to the large grain size in the microstructure. The API X70 steel base metal composed of carbon (0.045wt% C), silicon (0.17wt% Si), manganese (1.53wt% Mn), phosphorus (0.003wt% P), sulphur (<0.003wt% S), chromium (0.248wt% Cr), Nickel (<0.005wt% Ni), copper (<0.002wt% Cu), aluminum (0.018wt% Al), vanadium (0.014wt% V), molybdenum (0.110wt% Mo), titanium (0.022wt% Ti), (0.051wt%Nb), nitrogen (0.004wt% N), calcium (0.0022wt%), Boron (0.0026wt% B), it is therefore classified as low carbon steel alloying elements (Mn, V, Cr, Si, Ni, Mo and Cu) that help in the strengthening of the ferrite.

ii.   The experimental and numerical tensile value for plain specimen without defect was obtained to be 706.8 MPa and 1176.9 MPa respectively while for weld materials without defects 667.8 MPa was obtained experimentally and 646.92 MPa numerically. This shows agreement in the trend of results obtained experimentally and numerically. For that of compressive test, maximum stress obtained in plain and weld material without defect were 1200.4 MPa and 1300.2 MPa respectively were obtained experimentally which is in close agreement to the trend of the result obtained numerically as follows, maximum stress obtained in plain and weld material without defect were 1393.7 MPa and 1902.1 MPa respectively.

<center>42</center>

iii.   The tensile properties of parent and weld materials with artificial crack aspect ratio were determined. Ten specimens were tested for each material microstructure. The experimental as well as the numerical maximum stress for the parent materials were determined to be 706.8 MPa and 1776.9 MPa respectively at aspect ratio of 0.2. Meanwhile, the maximum stress of the weld materials was determined both experimentally and numerically to be 667.8 MPa and 646.93 MPa at aspect ratio of 0.2 and 1.0 respectively. The compressive properties of parent and weld materials with artificial crack aspect ratio were also determined both experimentally and numerically. The experimental as well as the numerical maximum stress for the parent materials were determined to be 1238.5 MPa and 1637.9 MPa at aspect ratios of 1.0 and 0.2 respectively. Meanwhile, the maximum stress of the weld materials was determined both experimentally and numerically to be 1500.5 MPa and 1929.9 MPa at aspect ratios of 1.0 and 0.2 respectively.

5.2   Recommendation

At the end of the study the following recommendations were made:

i.   Further research can be under taking to check the effect on a corrosion on API X70 steel since most pipeline steels are buried under ground or in the sea which are good environment for corrosion to occur.

ii.   Larger aspect ratio could also be investigated for the same material in future research

iii.   Mash analysis is recommended for the numerical procedure to get more accurate values near the experimental values.

REFERENCES

Adedipe, O. (2015). *Integrity of offshore structures* (Doctoral dissertation, Cranfield University).

Alengaram, U. J., Mahmud, H., & Jumaat, M. Z. (2011). Enhancement and prediction of modulus of elasticity of palm kernel shell concrete. *Materials & Design*, *32*(4), 2143-2148.

Anand S. (2021). Welding Defects - Classification, Causes and Remedies welding & NDT *(weldingandndt.com)*. lasted assessed October 28, 2021.

ASTM A751 -14. (2014). Standard Test Methods, Practices, and Terminology for Chemical Analysis of Steel Products.299.

Barsanti, L., Mannucci, G., Hillenbrand, H. G., Demofonti, G., & Harris, D. (2002, January). Possible use of new materials for high pressure linepipe construction: an opening on X100 grade steel. In *International Pipeline Conference* (Vol. 36207, pp. 287-298).

Belmonte, M. K., Mazziotta, J. C., Minshew, N. J., Evans, A. C., Courchesne, E., Dager, S. R., ... & Colamarino, S. A. (2008). Offering to share: how to put heads together in autism neuroimaging. *Journal of Autism and Developmental Disorders*, *38*(1), 2-13.

Dugstad, A. (2006). Fundamental Aspects of CO2 Metal Loss Corrosion Part I: Mechanism, in CORROSION/2006. *NACE International*.

Farhad, F., Zhang, X., Smyth-Boyle, D., & Khan, M. K. (2017). Evaluation of Simulated Corrosion Pits in X65 Steel. In *CORROSION 2017*. OnePetro.

Fikry, M. M., Ogihara, S., & Vinogradov, V. (2018). The effect of matrix cracking on mechanical properties in FRP laminates. *Mechanics of Advanced Materials and Modern Processes*, *4*(1), 1-16.

Guozhong, C., Kangda, Z., & Dongdi, W. (1996). Analyses of embedded elliptical cracks in finite thickness plates under uniform tension. *Engineering fracture mechanics*, *54*(4), 579-588.

Hillenbrand, H. G., Liessem, A., Kalwa, C., Erdelen-Peppler, M., & Stallybrass, C. (2008). Technological solutions for high strength gas pipelines. In *Proceedings of International Pipeline Steel Forum*.

Hillenbrand, H. G., Niederhoff, K. A., Amoris, E., Perdrix, C., Streisselberger, A., & Zeislmair, U. (1997, April). Development of Linepipe in Grades up to X 100. In *EPRG/PRC biennial joint technical meeting on linepipe research*.

Hudak Jr, S. J. (1981). Small crack behavior and the prediction of fatigue life. *Journal of Engineering Materials and Technology,* 103 26-35.

Idokoh, O J, (2016) Microstructure and mechanical properties of welds in pipeline steel, M.Sc. Thesis, *University of Saskatchewan Pp.18-21*

Ike, T. M., Adedipe, O., Abolarin, M. S., & Lawal, S. A. (2018, September). Mechanical Characterization of Welded API X70 Steel Exposed to Air and Seawater: A review. In *IOP Conference Series: Materials Science and Engineering* (Vol. 413, No. 1, p. 012034). IOP Publishing.

Ike, T. M., Adedipe, O., Lawal, S. A., Abolarin, M. S., & Olugboji, O. A. (2019). Investigation of the mechanical and microstructural properties of welded API X70 pipeline steel. *Arid Zone Journal of Engineering, Technology and Environment*, *15*(2), 342-354.

Kolawole, F. O., Kolawole, S. K., Agunsoye, J. O., Adebisi, J. A., Bello, S. A., & Hassan, S. B. (2018). Mitigation of corrosion problems in API 5L steel pipeline-a review. *Journal of Materials and Environmental Sciences*, *9*(8), 2397-2410.

Leonardo, B. G., Luiz, C. C., Rodrigo, V. B., & Soares, L. H. (2014). Microstructure and mechanical properties of two API steels for Iron ore pipelines. *Journal of Universidade federal de ouropreto, MG, Brazil*, *17*, 1516-1639.

Lin, X. B., & Smith, R. A. (1999). Finite element modelling of fatigue crack growth of surface cracked plates: Part II: Crack shape change. *Engineering Fracture Mechanics*, *63*(5), 523-540.

Llongueras, J. G., Hernandez, J., Munoz, A., Flores, J. M., & Duran-Romero, R. (2005, April). Mechanism of FeCO3 formation on API X70 pipeline steel in brine solutions containing CO2. In *CORROSION 2005*. OnePetro.

Miller, K. J. (1982). The short crack problem. *Fatigue & Fracture of Engineering Materials & Structures*, *5*(3), 223-232.

Milne, I., Ainsworth, R. A., Dowling, A. R., & Stewart, A. T. (1988). Assessment of the integrity of structures containing defects. *International Journal of Pressure Vessels and Piping*, *32*(1-4), 3-104.

Natividad, C., García, R., López, V. H., Falcón, L. A., & Salazar, M. (2017). Mechanical and metallurgical properties of grade X70 steel linepipe produced by non-conventional heat treatment. In *Characterization of Metals and Alloys* (pp. 3-11). Springer, Cham.

Newman, J. C., & Raju, I. S. (1979). Analyses of Surface Cracks in Finite Plate Under Tension or Bending Loads, NASA Tech.

Nonn, A., & Brauer, H. (2014, September). Establishing the correlation between Charpy impact energies for different sized specimens of modern pipeline steels. In *International Pipeline Conference* (Vol. 46124, p. V003T07A008). American Society of Mechanical Engineers.

Qin, X., Yan, W., Guo, X., & Gao, T. (2018). Effects of area, aspect ratio and orientation of rectangular nanohole on the tensile strength of defective graphene–a molecular dynamics study. *RSC advances*, *8*(31), 17034-17043.

Raju, I. S., & Newman, J. C. (1987). *Finite-element analysis of corner cracks in rectangular bars*. National Aeronautics and Space Administration, Langley Research Center.

Ravichandran, K. S. (1997). Effects of crack aspect ratio on the behavior of small surface cracks in fatigue: Part I. simulation. *Metallurgical and Materials Transactions A*, *28*(1), 149-156.

Ravichandran, K. S., & Larsen, J. M. (1997). Effects of crack aspect ratio on the behavior of small surface cracks in fatigue: Part II. Experiments on a titanium (Ti-8Al) alloy. *Metallurgical and Materials Transactions A*, *28*(1), 157-169.

Sachithanadam, M., & Joshi, S. C. (2016). Silica Aerogel Composites. *Engineering Materials*.

Schmitt, G. (2006). *Energy Security, National Security, and Natural Gas*. American Enterprise Institute.

Shamsuddoha, M., Islam, M. M., Aravinthan, T., Manalo, A., & Lau, K. T. (2013). Characterisation of mechanical and thermal properties of epoxy grouts for composite repair of steel pipelines. *Materials & Design (1980-2015)*, *52*, 315-327.

Shin, S. Y., Woo, K. J., Hwang, B., Kim, S., & Lee, S. (2009). Fracture-toughness analysis in transition-temperature region of Three American Petroleum Institute X70 and X80 pipeline steels. *Metallurgical and Materials Transactions A*, *40*(4), 867-876.

Smart, L., & Bond, L. J. (2016). Material property relationships for pipeline steels and the potential for application of NDE. In *AIP conference proceedings* (Vol. 1706, No. 1, p. 160003). AIP Publishing LLC.

Stalheim, D. G., & Muralidharan, G. (2006). The role of continuous cooling transformation diagrams in material design for high strength oil and gas transmission pipeline steels. In *International Pipeline Conference* (Vol. 42630, pp. 231-238).

Taylor D., & Knott J. F. (1981). Fatigue crack propagation behaviour of short cracks:the effetct of microstructure, *Fatigue & Fracture of Engineering Materials & Structures,* 4 147-155.

Vesga Rivera, W. (2014). "Structural Integrity of Steel Pipelines for CO2 Transport." PhD *Thesis, Cranfield University.*

Wang, Q., Chen, X., Jha, A. N., & Rogers, H. (2014). Natural gas from shale formation–the evolution, evidences and challenges of shale gas revolution in United States. *Renewable and Sustainable Energy Reviews*, *30*, 1-28.

Wang, W., Yan, W., Zhu, L., Hu, P., Shan, Y., & Yang, K. (2009). Relation among rolling parameters, microstructures and mechanical properties in an acicular ferrite pipeline steel. *Materials & Design*, *30*(9), 3436-3443.

Yap S., Alengaram U., & Jumaat, M. Z. (2016). The effect of aspect ratio and volume fraction on mechanical properties of steel fibre-reinforced oil palm shell concrete, *journal of civil engineering and management,* vol. 22(2): 168-177

Zhao, M. C., Yang, K., & Shan, Y. Y. (2003). Comparison on strength and toughness behaviors of microalloyed pipeline steels with acicular ferrite and ultrafine ferrite. *Materials Letters*, *57*(9-10), 1496-1500.

Zhuang, L. I., Di, W. U., & Wei, L. Ü. (2012). Effects of rolling and cooling conditions on microstructure and mechanical properties of low carbon cold heading steel. *Journal of Iron and Steel Research, International*, *19*(11).

CERTIFICATE OF ANALYSIS

Date: 26/02/20

N°:

Ref. Alloy: API 5L X 70

Customer: ERINFOLAMI O. ISAAC

Operator: YUSUF

Order: 035/17

This is to certify that the goods

Goods:

Sample: P 43
Cast: B2408094
COIL NO: 365

have this chemical analysis:

	C%	Si%	Mn%	P%	S%	Cr%	Mo%	Ni%	Nb%
Report	0.042	0.164	1.599	0.013	0.004	0.231	0.149	0.005	0.056
Ref. MIN	—	—	—	—	—	—	—	—	—
Ref. MAX	—	—	—	—	—	—	—	—	—

	Al%	Cu%	Co%	B%	Ti%	V%	W%	Mg%	Ca%
Report	0.042	0.003	<0.002	:0.0005	0.020	0.029	0.005	0.0014	0.0035
Ref. MIN	—	—	—	—	—	—	—	—	—
Ref. MAX	—	—	—	—	—	—	—	—	—

	Ce%	La%	As%	Pb%	Sn%	Sb%	Te%	Zn%	Zr%
Report	<0.002	0.013	<0.005	0.013	<0.001	0.018	<0.001	<0.001	0.003
Ref. MIN	—	—	—	—	—	—	—	—	—
Ref. MAX	—	—	—	—	—	—	—	—	—

	N%	Fe%							
Report	<0.003	97.578							
Ref. MIN	—	—							
Ref. MAX	—	—							

Notes :

48